CEAS Space Journal
https://doi.org/10.1007/s12567-019-00278-4

ORIGINAL PAPER

Damping of piezoelectric space instruments: application to an active optics deformable mirror

David Alaluf[1,2] · Bilal Mokrani[3,4] · Kainan Wang[1] · André Preumont[1]

Received: 7 July 2019 / Revised: 4 September 2019 / Accepted: 6 September 2019

Abstract
This paper presents the shunt damping of a unimorph piezoelectric mirror intended to be used as an active secondary corrector in future space telescopes. We propose to take advantage of the actuation capability of the piezoelectric mirror, to increase its natural damping during the critical launch phase of the spacecraft. The piezoelectric actuators, intended to be used for active optics, are shunted on a passive resistive and inductive RL circuit during the launch operation. The proposed concept is verified numerically and experimentally on a piezoelectric deformable mirror prototype, developed on behalf of the European Space Agency. We show that the shunt damping significantly reduces the response of the most critical mode of the mirror (− 23 dB) as well as the stress in the mirror when subjected to a typical vibro-acoustic launch load. This reduces the risk of damaging the mirror during the delicate launch phase, without increasing the complexity of the design.

Keywords Active optics · Adaptive optics · Deformable mirrors · Space telescopes · Piezoelectric shunt · Vibration damping

1 Introduction

Launch vehicles have limited mass and size payload which restricts the transport of large space telescopes. This limitation progressively leads to the development of stowable primary reflectors with very low aerial density, such as segmented primary mirrors, lenticular pressure stiffened membranes and doubly curved form stiffened elastic shells as shown in Fig. 1 [1]. To guarantee an optimal operation and preserve a precise pointing, large lightweight space telescopes will involve active systems aiming at compensating for optical aberrations. Among these systems, we find active shaping and cophasing of segmented mirrors (e.g. the James Webb Space Telescope) as well as deformable mirrors (DM), already successfully used in most of the state-of-the-art terrestrial telescopes to cope with atmospheric turbulence [2]. More recently, the space community has been interested in extending the use of deformable mirrors in space telescopes to compensate for aberrations induced by deployment imprecision, manufacturing errors, gravity release and thermal distortion. Thanks to its simple architecture, the piezoelectric unimorph technology can offer high reliability; hence it is a good candidate for space applications as shown in [3, 4].

In addition to highly stringent requirements in terms of optical surface quality, weight and thermal stability, the design of a deformable mirror relies on its ability to generate some specific shapes (corresponding to the expected optical aberrations) with a relatively high stroke, typically of 5–10 µm. These specifications determine the number and the shape of the piezoelectric actuators. As any part of the payload, the DM must survive to the strong vibro-acoustic loads occurring during the launch of the spacecraft. Obviously, the lower the stiffness of the DM, the better the amplitude deformation one can achieve, but the more vulnerable is the DM to mechanical vibrations. As an example, a unimorph piezoelectric deformable mirror has been presented in [5];

✉ David Alaluf
David.Alaluf@esa.int

✉ Bilal Mokrani
Bilal.Mokrani@asml.com

1 Department of Control Engineering and System Analysis, Université Libre de Bruxelles, Brussels, Belgium

2 ESA/STEC, Optoelectronics Section, Noordwijk, The Netherlands

3 Department of Mechanical, Materials and Aerospace Engineering, University of Liverpool, Liverpool, UK

4 Mechatronics Department, ASML, Veldhoven, The Netherlands

Published online: 25 September 2019

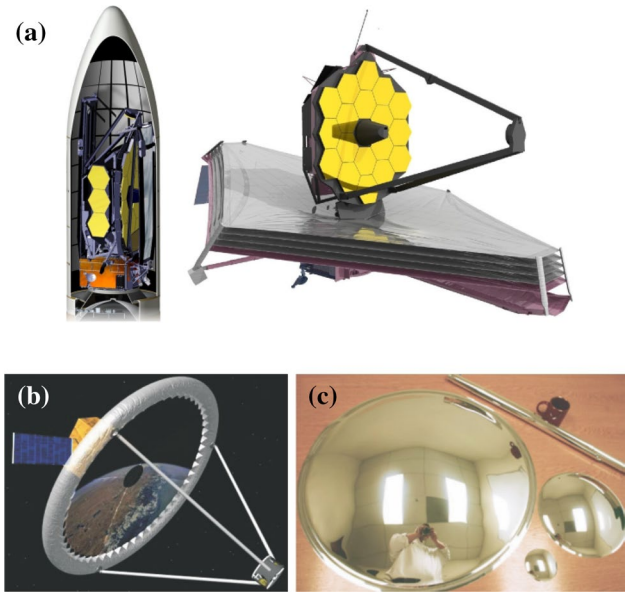

Fig. 1 **a** James Webb Space Telescope (with an aeral density of 20 kg/m^2), folded in the launcher and after deployment. **b**, **c** Future generations of very large ($D > 10$ m) and ultra-lightweight space reflectors with an areal density of 3 kg/m

it passed all the space qualification campaign except one of the vibration tests, where the supporting arms failed [6].

This paper shows how one can take advantage of the actuation capabilities of a unimorph deformable mirror to further increase its natural damping during the delicate launch phase of the spacecraft. The proposed concept is demonstrated on a deformable mirror we developed in the framework of a GSTP program ("BIALOM") on behalf of the European Space Agency (ESA) [7]. The performance of the mirror has already been extensively presented in [4]. It has been shown that the mirror is already fully compliant with all the goals sets by ESA (from mechanical and optical point of view), corresponding to a Technology Readiness Level of 4 (TRL 4). In the present paper, we go further and propose to shunt the actuators of the deformable mirror, intended to be used for the shaping of the mirror once deployed, on passive electrical shunts [8, 9], only during the launch of the spacecraft. As shown in Sects. 4 and 5, this makes it possible to reduce the dynamic stress experienced by the mirror due to the severe vibro-acoustic loads and to significantly damp the most critical mode of the mirror. Therefore, it allows improving the safety margins of the DMs, which are generally fragile and soft, at a minimal cost and mass since the damping is achieved by means of the piezoelectric actuators which will be used for the shape control. This method might be particularly useful for large and thin deformable mirrors since the first resonance frequency of the mirror is decreasing as the square of the mirror diameter and as the third power of its thickness. Note also that the RL shunt damping would also allow using deformable mirror configurations which otherwise may not survive to the launch loads (e.g. flexible configurations which would fail a vibration qualification test). A similar study was conducted numerically on a silicon carbide primary mirror (M1) for space telescopes [10]; the authors compared various passive and active vibration alleviation techniques against vibro-acoustic loads and concluded that increasing the damping of the M1 during launch would allow to use better designs of deformable mirrors. Here, we extend these results by implementing numerically and experimentally the piezoelectric resistive and inductive RL shunt on a deformable mirror. Among the existing shunt damping techniques, we select the passive RL shunt for its simplicity and efficiency [11, 12]. Although highly sensitive to the variation of the targeted mode resonance frequency, the RL shunt remains efficient for piezoelectric structures with a high electromechanical coupling factor, which is representative of the considered mirror [13]. Other semi-active techniques, such as synchronized switch damping on inductor [14], and negative capacitance [15], could be also considered at the expense of a power source and an accurate switching algorithm. The goal of this study is not to validate all of them, but to demonstrate the feasibility of using piezoelectric shunts during the launch to improve the structural damping of the DM.

The paper is organized as follows: Sect. 2 describes the deformable mirror, Sect. 3 reminds the main elements of piezoelectric shunt damping theory, Sect. 4 shows numerically the performance expected based on typical vibro-acoustic spectra. Finally, Sect. 5 validates experimentally the benefit of using the RL shunt.

2 Piezoelectric mirror

2.1 Design

The mirror consists of a single-crystal Si wafer (76.2 mm diameter, 500 µm thickness) covered with a high-quality aluminium optical coating on the front side to reach a reflectivity higher than 97% for wavelengths around 633 nm. The rear face of the wafer is covered with an aluminium ground electrode on which is glued a thin PZT patch (50 mm diameter, 200 µm thickness) operating in d_{31} mode [16–18]. The commercial PZT patch (PIC-252 from PI Ceramic) is supplied with a single thin metallic Cu/Ni electrode of ~ 1 µm thickness. Before the gluing of the PZT patch on the Si mirror, the desired electrode pattern is obtained by laser ablation of the continuous Cu/Ni electrode (with a gap of 200 µm to avoid arcing within the PZT). A network of 25 independent electrodes is used to control the mirror shape. The electrodes are arranged in a keystone pattern, modified to include tracks and outer pads to bring all the electrical connections at the

periphery of the PZT. This allows to reject potential defects induced by the wires (local print-through and depolarizing of the PZT material during the soldering process) outside the optical pupil. Finite elements simulations showed that the tracks do not jeopardize the ability to meet the specifications (particularly with thin tracks 200 µm width). A cross-section of the DM is sketched in Fig. 2. It describes the various layers composing the deformable mirror as well as their respective thicknesses. To account for the fact that PZT cannot be actuated with plus and minus voltages, the PZT wafer was glued (with space-qualified glue EPO-TEK-301) under voltage according to the technique described in [19], so that the initial shape of the mirror is concave and the normal operating range of the deformable mirror is symmetric with respect to an initial bias necessary to remove the initial concave curvature.

The deformable mirror is connected to a lightweight support plate through an active isostatic mount. The main challenges in the design of the isostatic support lie in meeting the conflicting requirements: (1) the support must allow thermal differential expansion between the mirror and its supporting structure; but (2) the mirror assembly must withstand the strong accelerations associated with the space qualification, which requires a strong connection between the mirror and its support, and a natural frequency large enough. The adopted solution consists of three active feet, each composed of a flexible blade and a space-qualified position linear actuator (Cedrat APA 50XS), allowing control of the rigid-body motion of the mirror. In this way, the isostatic mount has a negligible impact on the deformation of the mirror and provides the best authority with respect to other mounts (e.g. a clamped design). The demonstrator is shown in Fig. 3.

2.2 Finite element model

The whole deformable mirror, including the active feet, has been analysed with the Finite Elements software SAMCEF as shown in Fig. 4. Standard triangular and quadrangular plate/shell elements are used to mesh the deformable mirror and the flexible blades. Volume elements are used to represent the interface parts between the mirror and the blades.

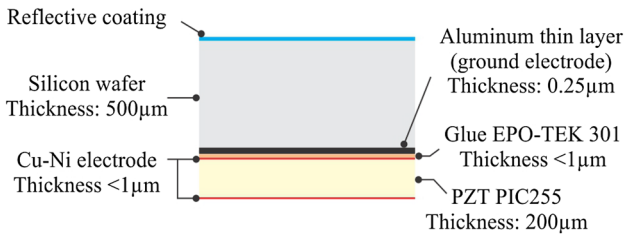

Fig. 2 Material layers composing the unimorph deformable mirror and their corresponding thicknesses

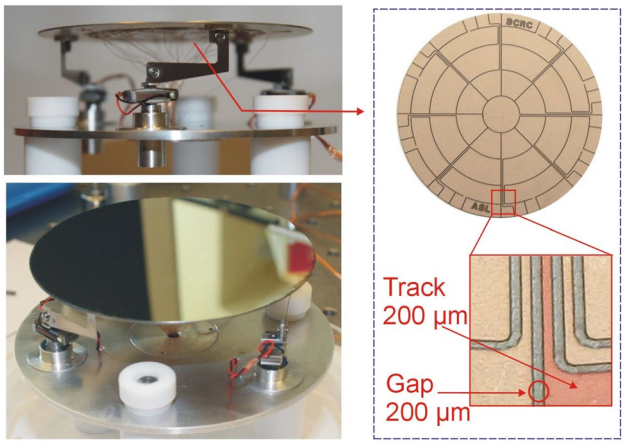

Fig. 3 Overview of the experimental setup of an active bimorph piezoelectric mirror. The total mass of the demonstrator is 54.8 g

The mesh is chosen with an adequate density to model all the local effects accurately. The mechanical behaviour of the mirror is modelled using multilayered Mindlin formulation. The thickness and material properties of each layer are defined independently. The single-crystal silicon wafer is cut in the [1,0,0] plane; although weakly orthotropic, numerical models with isotropic average properties have been found sufficient for numerical predictions. The PZT actuators are modelled by a layer with the properties of a piezoelectric material [21, 22].

Note that the mirror is bonded to the active feet by means of a double sided adhesive tape (that meets the vacuum requirements for environmental tests). The adhesive tape allows a lower in-plane and vertical stiffness, and acts as an isolator. The Young's modulus of the adhesive tape was identified experimentally. The numerical model allows implementing easily combinations of an arbitrary set of layers to represent any design option that may be worth to study. The finite

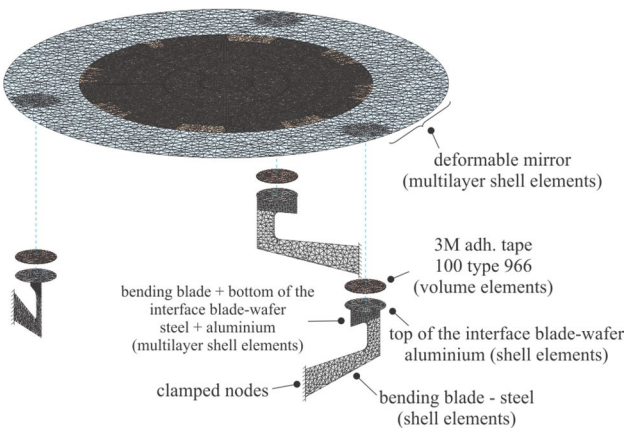

Fig. 4 Exploded view of the Full FE model

element model is then exported to MATLAB, where a state space model is built, with as inputs the mechanical forces and the electrical charges in the piezoelectric transducers, while the outputs are the nodes displacements and the voltages generated by the piezoelectric transducers. A Craig–Bampton reduction is used, where the first 40 modes are kept. A modal damping $\xi = 1\%$ is considered for all the modes; this value has been identified experimentally on various prototypes.

2.3 Experimental modal analysis

Figure 5 shows the result of an experimental modal analysis conducted on the mirror without RL shunt damping. The measurement was performed for a bandwidth between 100 Hz and 1600 Hz. The mirror is excited by the central electrode, while a non-contact 2D Polytec scanner is used as a sensor. The lowest eigenfrequency, $f_1 = 243$ Hz, corresponds to a piston mode, likely to be due to the tape at the connection between the flexible blades and the mirror. The first internal flexible mode occurs at $f = 771$ Hz, while the second appears at 1244 Hz, with an inherent modal damping of about 1%. The shunt damping will be targeted on this mode.

3 Theory of RL shunt damping

Consider the single degree of freedom piezoelectric system of Fig. 6, shunted in series on a resistor R and an inductor L. Its dynamics is governed by [20]:

$$M\ddot{x} + K_a x = \frac{d_{33}K_a}{C\left(1-k^2\right)}Q, \tag{1}$$

$$L\ddot{Q} + R\dot{Q} + \frac{1}{C\left(1-k^2\right)}Q = \frac{d_{33}K_a}{C\left(1-k^2\right)}x, \tag{2}$$

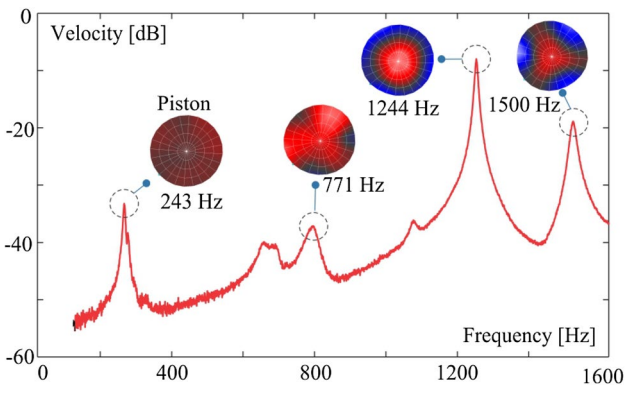

Fig. 5 Average spectrum (magnitude of the velocity) of the frequency response and the corresponding mode shapes of the deformable mirror

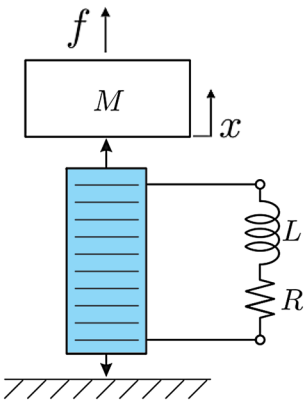

Fig. 6 Single degree of freedom

where M is the mass, x is its displacement, Q is the electrical charge, K_a is the transducer stiffness with short-circuited electrodes, C is its capacitance with free–free mechanical boundary condition, d_{33} is the piezoelectric constant, and $k^2 < 1$ is the electromechanical coupling factor which quantifies the ability of the transducer to convert mechanical energy to electrical energy and vice versa.

The system of Fig. 6, described with Eqs. (1, 2), consists of two coupled oscillators, such that the electrical circuits oscillator absorbs the vibration energy of the mechanical oscillator. We define the resonance frequency ω_e and damping ξ_e of the electrical circuit as:

$$\omega_e = \frac{1}{\sqrt{LC\left(1-k^2\right)}} \quad \text{and} \quad 2\xi_e\omega_e = \frac{R}{L}. \tag{3}$$

The piezoelectric transducer, shunted on the inductor L and the resistor R, behaves in a way very similar to the celebrated tuned mass absorber. The resistor is used to dissipate the absorbed energy, it can be mounted, either in series or in parallel. Depending upon the frequency content of the disturbance, the tuning can be made in two ways [23, 24]:

(a) Equal peak design:

The RL circuit is tuned to minimize the H_∞ norm (i.e. the maximum) of the frequency response function (FRF) between the displacement of the mass and an external disturbance force. This design is usually referred to as the equal peak design because it results in a double peak with equal amplitudes of the frequency response, as shown in Fig. 7. To maximize the energy absorption, the inductor is tuned such that the electrical resonance frequency ω_e^* matches the mechanical resonance frequency Ω_i. The optimal parameters are:

$$\frac{\omega_e^*}{\omega_i} = \frac{1}{\sqrt{1-k^2}} \quad \text{or} \quad \frac{\omega_e^*}{\Omega_i} = 1, \tag{4}$$

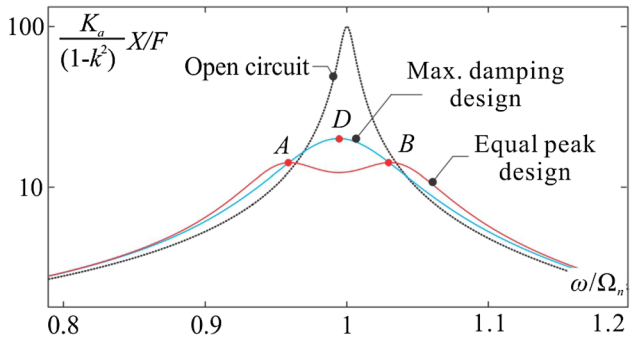

Fig. 7 RL shunt tuning of a single degree of freedom system: FRF with and without RL shunt

and

$$\xi_e^* = \sqrt{3/8}k, \tag{5}$$

where Ω_i and ω_i are, respectively, the resonance frequencies of the targeted mode with open-electrodes, and with short-circuited electrodes. The equal peak design is the most commonly used.

(b) Maximum damping (stability) design

The RL circuit is tuned to maximize the damping of the targeted mode, and thus the stability of the system. The optimal tuning of the RL circuit is achieved by choosing the electrical resonance frequency ω_e^* as:

$$\frac{\omega_i \omega_e^*}{\Omega_i} = 1 \quad \text{or} \quad \frac{\omega_e^*}{\omega_i} = \frac{1}{1-k^2}, \tag{6}$$

and the electrical damping ξ_e^* as

$$\xi_e^* = k. \tag{7}$$

Observe that the above tuning equations depends merely on four measurable parameters: the inherent piezoelectric capacitance C, the resonance frequencies of the targeted mode with open and short-circuited electrodes, Ω_i and ω_i, and the electromechanical coupling factor k. Therefore, the aforementioned tuning rules apply directly to any piezoelectric structure, provided these four tuning parameters are available. Note also that, for a multi-degree of freedom system, the generalized electromechanical coupling factor K_i, associated with a specific mode i, should be used instead of k; it is defined as:

$$K_i^2 = 1 - \frac{\omega_i^2}{\Omega_i^2} \tag{8}$$

4 Numerical simulations

The piezoelectric shunt damping of the deformable mirror, is first implemented numerically on the model described in Sect. 2.2. The piezoelectric patches are connected in parallel, so that they act as a single transducer [11]; they are then shunted on a resistor R and an inductor L, mounted in series as shown in Fig. 8. The shunt is targeted on the second flexible mode (with defocus-like shape), with resonance frequency $\omega_2 = 1244$ Hz. This mode is the most likely to be exited under a launching environment, as it exhibits a uniform curvature (almost axisymmetric shape) and has the highest amplitude if the mirror is excited by a uniform dynamic pressure (which is true for the small surface of the wafer), or by a seismic excitation transmitted through the three supporting legs. When the structure vibrates according to this mode, the piezoelectric patches generate in-phase electrical charges, proportional to the strain at their corresponding positions. Therefore, one can either use the piezoelectric patches independently by shunting each of them on an independent RL branch, which results in 24 circuits, or connect them in parallel as a single patch, which requires a single RL branch. The second configuration is preferred since it simplifies the integration, and requires a single circuit with a smaller inductor compared to the independent configuration. The generalized electromechanical coupling factor K_i, associated with the targeted mode is $K_2 = 24\%$, it is calculated using Eq. (8).

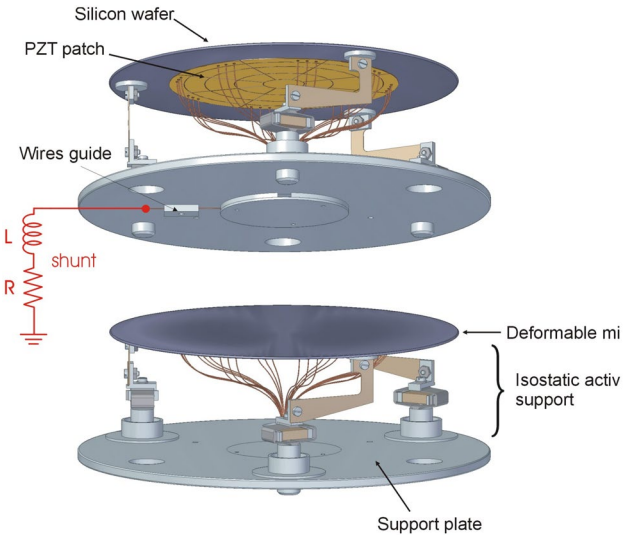

Fig. 8 CAD view of the deformable mirror. All the piezoelectric patches are connected in parallel on a single passive RL shunt

Figure 9 compares the frequency response function (FRF) between the voltage applied to the central patch and the velocity computed at one point on the mirror surface: (1) with open electrodes; and (2) when the 24 patches are connected in parallel and shunted on a single RL circuit. The optimal inductor and resistor are computed according to Eqs. (4, 5). The shunt reduces the peak response of the mirror by a factor 10 (or 23 dB); this is possible thanks to the

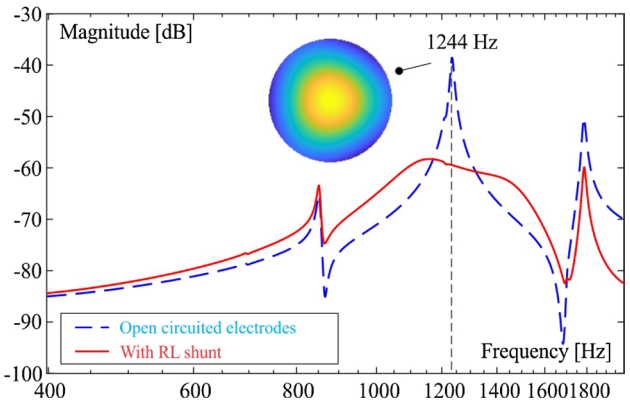

Fig. 9 Numerical results: FRF of the mirror computed between the voltages applied to the central patch and the velocity of a point on the mirror surface, with and without RL shunt

high value of the electromechanical coupling factor associated with the targeted mode.

4.1 Response to support vibrations

The disturbing vibration is defined in terms of acceleration power spectral density and applied on the active feet of the DM, in the vertical direction. A typical spectrum [10], normalized to 20 g, is used as shown in Fig. 10.

The root mean square (RMS) of the upper skin Von Mises stress in the deformable mirror is computed using the SPECTRAL module SAMCEF software [25]. The result is shown in Fig. 11 with and without the RL-shunt damping.

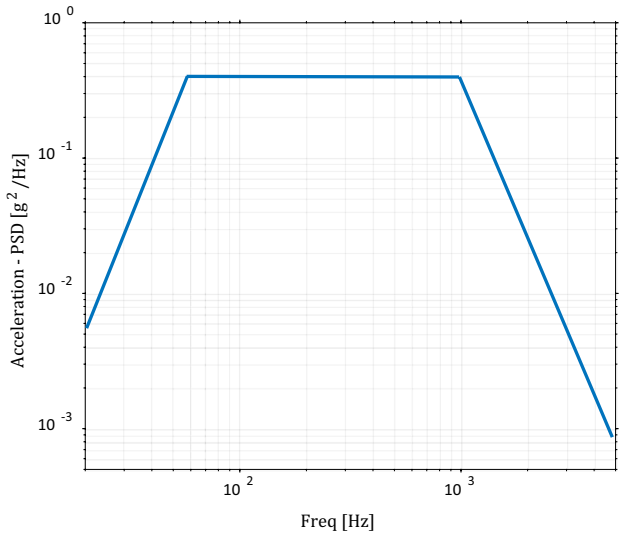

Fig. 10 Prescribed power spectrum density of the vibration acceleration from the supports

As expected, damping the critical mode reduces the stress experienced by the mirror. In particular, the stress at the most critical locations is attenuated by almost a factor 4, which reduces significantly the risk of failure.

4.2 Response to acoustic pressure

The acoustic load is applied over the whole surface of the mirror. The simulation considers a dynamic pressure on the mirror surface as shown in Fig. 12. The normalization is done to ensure an overall sound pressure level of 150 dB.

Due to the small size of the mirror, the pressure is assumed to be uniformly distributed. Figure 13 shows the computed stress (RMS) in the mirror. Once again, it shows the benefit of the shunt damping, allowing a reduction of the stress experienced at the most critical points by a factor larger than two.

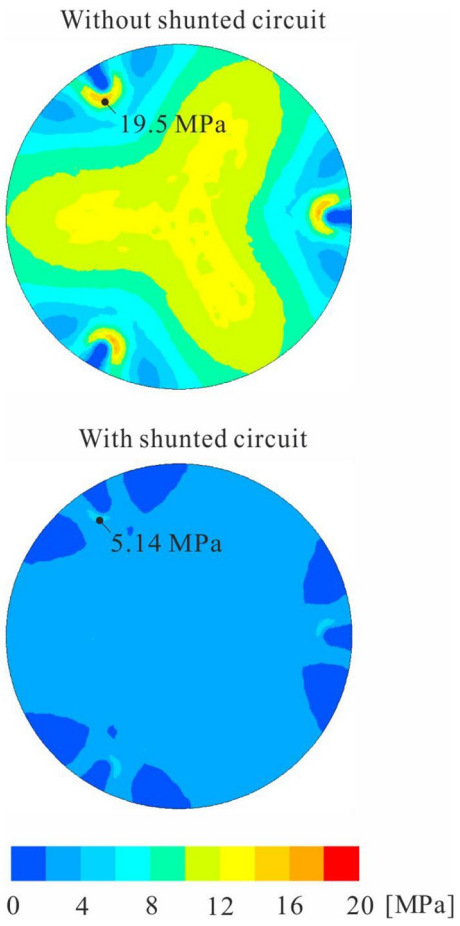

Fig. 11 Upper skin Von Mises stress (RMS) caused by support acceleration, with and without shunt damping

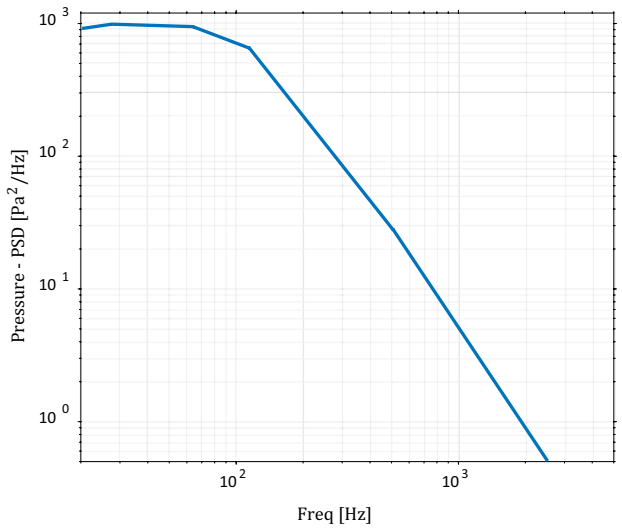

Fig. 12 Power spectrum density of the dynamic pressure from the acoustic background

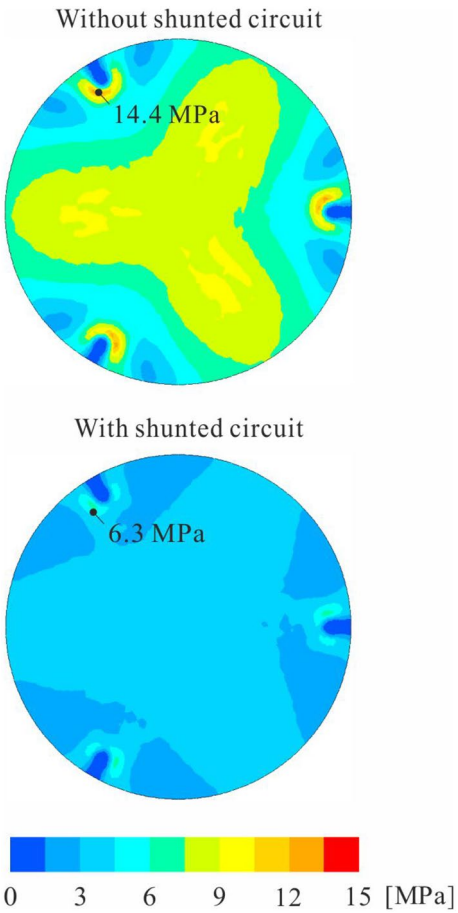

Fig. 13 Upper skin Von Mises stress (RMS) on DM surface caused by acoustic excitation, with and without shunt damping

5 Experimental validation

The RL shunt damping is implemented experimentally on the deformable mirror of Fig. 3. To facilitate the tuning of the shunt components, a synthetic inductor was used instead of a passive inductor. It consists of an active circuit employing operational amplifiers OPA445; its equivalent circuit is shown in Fig. 14. The mode at 1244 Hz is considered for the damping.

The generalized electromechanical coupling factor K_i associated to the targeted mode is obtained using Eq. (8), where $\Omega_n = 1244$ Hz and $\omega_n = 1196$ Hz, resulting in maximum damping of the targeted mode of about $\xi_i = K_i/2 = 14\%$. Given the value of the total electrical capacitance of the piezoelectric patches $C = 140$ nF (measured using an impedance meter), one can easily find the optimal tuning of the shunt by simply using Eqs. (4) and (5), according to the Equal Peak Design.

The required inductor is about $L = 120$ mH while the required resistor is $R = 300\,\Omega$. These values of the electrical components can be considered very small and easily realizable; however, although the inductor has a small value, it must be sized to handle all the electric charges generated by the piezoelectric transducer and avoid any saturation. Its physical size will be mainly defined by the vibration level and not merely by its value. Figure 15 shows the frequency response function of the mirror measured between the voltage applied to the central patch and the velocity measured at one point of the mirror by means of a laser vibrometer: (1) when the electrodes are open; (2) when they are short circuited; and (3) when all the patches are connected in parallel and shunted on a single RL circuit. The figure shows a reduction of about 23 dB (a factor of 14) of the peak response of the targeted mode, resulting in a reduction in the RMS value of the response by 34%.

Remark: If another mode would have been targeted for the damping, the piezoelectric patches could be rearranged to match the targeted mode shape, in a similar manner to a

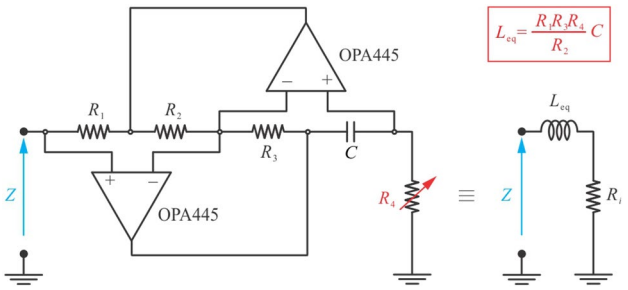

Fig. 14 Antoniou circuit simulating a perfect inductance (synthetic inductor); R_i is the internal resistance of the circuit, it is zero when perfect operational amplifiers are used [26]

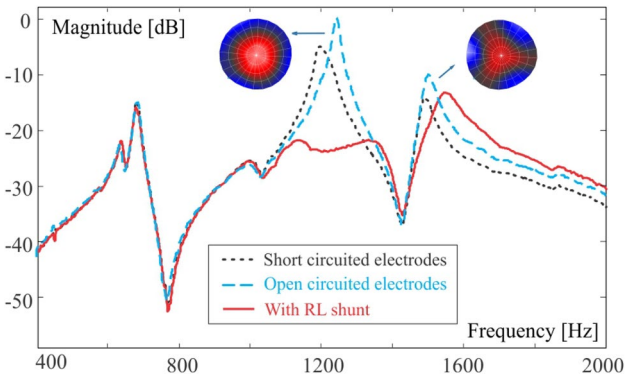

Fig. 15 Frequency response function of the mirror measured between the voltages applied to the central patch and the velocity measured at one point of the mirror: when the electrodes are open when they are short circuited, and when all the patches are connected in parallel and shunted on a single RL circuit

modal filter [27, 28]; this would not affect the needed size of inductor while it preserves the shunt performance. It is also possible to organize the piezoelectric patches with a more elaborated multi-degree of freedom circuit, in such a way that the "electrical" resonance frequencies and mode shapes match several targeted structural modes, see e.g. [29] and [30]; in this case, several inductors are required.

6 Conclusion

In this paper, we present a method to increase the natural damping of a deformable piezoelectric mirror during the delicate launch phase of the spacecraft, without increasing the complexity of the mirror. To do so, we propose to take advantage of the piezoelectric actuators, intended to be used for adaptive optics once the telescope is deployed. By connecting them to a passive RL circuit during the launch operation, we show numerically that (1) the stress level is significantly reduced for both a random seismic excitation as well as an acoustic pressure and (2) that the amplitude of the most critical mode is reduced by 23 dB (i.e. a factor 10). This is then confirmed experimentally on a deformable mirror previously manufactured in the framework of an ESA project. The demonstrated concept is intended to be used in future missions of the European Space Agency.

Acknowledgements The authors thank prof. M. Horodinca and prof. I. Romanescu from University of Ghorghe Asachi, Iasi, Romania, for the realization of the experimental setup. This research was partially supported by "Région Wallonne", in the framework of "MECATEC-M4" project, and by the European Space Agency (ESA) in the framework of BIALOM project. Kainan Wang is supported by the China Scholarship Council. The support of Centre Spatial de Liège is highly appreciated.

References

1. Jenkins, C.H.: Progress in Astronautics and Aeronautics: Gossamer Spacecraft: Membrane And Inflatable Structures Technology for Space Applications, vol. 191. American Institute of Aeronautics and Astronautics, Reston (2001)
2. Madec, P.-Y.: Overview of deformable mirror technologies for adaptive optics and astronomy. In: Ellerbroek, Marchetti, Véran, (eds.) Adaptive Optics Systems III, vol. 8447. SPIE, Bellingham (2012)
3. Alaluf, D.: Piezoelectric mirrors for adaptive optics in space telescopes, PhD thesis. Université Libre de Bruxelles, Active Structures Laboratory (2016)
4. Alaluf, D., Bastaits, R., Wang, K., Horodinca, M., Martic, G., Mokrani, B., Preumont, A.: Unimorph mirror for adaptive optics in space telescopes. Appl. Opt. **57**(15), 3629–3638 (2018)
5. Rausch, P., Verpoort, S., Wittrock, U.: Unimorph deformable mirror for space telescopes: design and manufacturing. Opt. Express **23**(15), 19469–19477 (2015)
6. Rausch, P., Verpoort, S., Wittrock, U.: Unimorph deformable mirror for space telescopes: environmental testing. Opt. Express **24**(2), 1528–1542 (2016)
7. Bimorph Adaptive Large Optical Mirror Demonstrator. ESA/ESTEC contract Nº 400010294/11/NL/CP
8. Forward, R.L.: Electronic damping of vibration in optical structures. Appl. Opt. **18**(5), 690–697 (1979)
9. Forward R. L.: Electromechanical transducer-coupled mechanical structure with negative capacitance compensation circuit. US Patent 4158787 (1979)
10. Cohan, L.E., Miller, D.W.: Vibroacoustic launch analysis and alleviation of lightweight active mirrors. Opt. Eng. **50**(1), 013002 (2011)
11. Hagood, N.W., von Flotow, A.: Damping of structural vibrations with piezoelectric materials and passive electrical networks. J. Sound Vib. **146**(2), 243–268 (1991)
12. Hollkamp, J.J.: Multimodal passive vibration suppression with piezoelectric materials and resonant shunts. J. Intell. Mater. Syst. Struct. **5**(1), 49–57 (1994)
13. Mokrani, B., Burda, I., Preumont, A.: Adaptive Inductor for Vibration Damping in Presence of Uncertainty, in Smart Structures and Materials. Springer, NY (2017)
14. Richard C., Guyomar D., Audigier D. Bassaler H.: Enhanced semi passive damping using continuous switching of a piezoelectric device on an inductor. Proceeding of the SPIE International Symposium on Smart Structures and Materials, Newport Beach, CA, United States, pp 288–300 (2000)
15. Mokrani, B., Rodrigues, G., Burda, I., Bastaits, R., Preumont, A.: Synchronized switch damping on inductor and negative capacitance. J. Intell. Mater. Syst. Struct. **23**(18), 2065–2075 (2012)
16. Adelman, N.T.: Spherical mirror with piezoelectrically controlled curvature. Appl. Opt. **16**, 3075–3076 (1977)
17. Kokorowski, S.A.: Analysis of adaptive optical elements made from piezoelectric bimorphs. J. Opt. Soc. Am. **69**, 181–187 (1979)
18. Steinhaus, E., Lipson, S.: Bimorph piezoelectric flexible mirror. J. Opt. Soc. Am. **69**, 478–481 (1979)
19. Bastaits, R., Alaluf, D., Horodinca, M., Romanescu, I., Burda, I., Martic, G., Rodrigues, G., Preumont, A.: Segmented bimorph mirrors for adaptive optics: segment design and experiment. Appl. Opt. **53**(29), 6635–6642 (2014)
20. Preumont, A.: Mechatronics, Dynamics of Electromechanical and Piezoelectric Systems. Springer, NY (2006)
21. Piefort, V., Loix, N., Preumont, A.: Modeling of piezolaminated composite shells for vibration control, ESA Conference on Spacecraft Structures, Materials and Mechanical Testing, ESA SP-428, Braunschweig, Germany (1999)

22. Piefort, V.: Finite element modeling of piezoelectric active structures, PhD Thesis, Université Libre de Bruxelles, Active Structures Laboratory (2001)
23. Asami, T., Nishihara, O., Baz, A.M.: Analytical solutions to H_∞ and H_2 optimization of dynamic vibration absorbers attached to damped linear systems. J. Vib. Acoust. **124**(2), 284–295 (2002)
24. Soltani, P., Kerschen, G., Tondreau, G., Deraemaeker, A.: Piezoelectric vibration damping using resonant shunt circuits: an exact solution. Smart Mater. Struct. **23**(12), 125014 (2014)
25. Preumont, A., Piefort, V.: Predicting high-cycle fatigue life with finite elements. ASME J. Vib. Acoust. **16**, 245–248 (1994)
26. Philbrick Researches Inc: Application Manual for Computing Amplifiers for Modeling, Measuring, Manipulating and Much Else. Nimord Press, Boston (1965)
27. Mokrani, B., Bastaits, R., Horodinca, M., Romanescu, I., Burda, I., Viguié, R., Preumont, A.: Parallel piezoelectric shunt damping of rotationally periodic structures. Adv. Mater. Sci. Eng. **2015**, Article ID 162782 (2015)
28. Preumont, A.: Vibration Control of Active Structures: an Introduction, vol. 246. Springer, NY (2018)
29. Tang, J., Wang, K.W.: Vibration control of rotationally periodic structures using passive piezoelectric shunt networks and active compensation. J. Vib. Acoust. **121**(3), 379–390 (1999)
30. Lossouarn, B., Deü, J.F., Aucejo, M., Cunefare, K.A.: Multimodal vibration damping of a plate by piezoelectric coupling to its analogous electrical network. Smart Mater. Struct. **25**(11), 115042 (2016)